THE JOURNAL OF BIOLOGICAL CHEMISTRY
Vol. 279, No. 43, Issue of October 22, pp. 44785–44794, 2004
Printed in U.S.A.

Establishment and Characterization of Cultured Epithelial Cells Lacking Expression of ZO-1*

Received for publication, June 11, 2004, and in revised form, July 26, 2004
Published, JBC Papers in Press, July 30, 2004, DOI 10.1074/jbc.M406563200

Kazuaki Umeda‡§, Takeshi Matsui§, Mayumi Nakayama§, Kyoko Furuse§, Hiroyuki Sasaki§¶, Mikio Furuse‡, and Shoichiro Tsukita‡‖

From the ‡Department of Cell Biology, Kyoto University Faculty of Medicine, Yoshida-Konoe, Sakyo-ku, Kyoto 606-8501, Japan, the §KAN Research Institute Inc., Kyoto Research Park, Chudoji, Shimogyo-ku, Kyoto 600-8815, Japan, and the ¶Department of Molecular Cell Biology, Institute of DNA Medicine, The Jikei University School of Medicine, Nishi-Shinbashi, Minato-ku, Tokyo 105-8461, Japan

In well polarized epithelial cells, closely related ZO-1 and ZO-2 are thought to function as scaffold proteins at tight junctions (TJs). In epithelial cells at the initial phase of polarization, these proteins are recruited to cadherin-based spotlike adherens junctions (AJs). As a first step to clarify the function of ZO-1, we successfully generated mouse epithelial cell clones lacking ZO-1 expression (*ZO-1*−/− cells) by homologous recombination. Unexpectedly, in confluent cultures, *ZO-1*−/− cells were highly polarized with well organized AJs/TJs, which were indistinguishable from those in *ZO-1*+/+ cells by electron microscopy. In good agreement, by immunofluorescence microscopy, most TJ proteins including claudins and occludin appeared to be normally concentrated at TJs of *ZO-1*−/− cells with the exception that a ZO-1 deficiency significantly up- or down-regulated the recruitment of ZO-2 and cingulin, another TJ scaffold protein, respectively, to TJs. When the polarization of *ZO-1*−/− cells was initiated by a Ca^{2+} switch, the initial AJ formation did not appear to be affected; however, the subsequent TJ formation (recruitment of claudins/occludin to junctions and barrier establishment) was markedly retarded. This retardation as well as the disappearance of cingulin were rescued completely by exogenous ZO-1 but not by ZO-2 expression. Quantitative evaluation of ZO-1/ZO-2 expression levels led to the conclusion that ZO-1 and ZO-2 would function redundantly to some extent in junction formation/epithelial polarization but that they are not functionally identical. Finally, we discussed advantageous aspects of the gene knockout system with cultured epithelial cells in epithelial cell biology.

The tight junction (TJ)[1] is one type of cell-to-cell adhesion structure in epithelial cells. TJs constitute the epithelial junctional complex together with adherens junctions (AJs) and desmosomes and are located in the most apical part of the complex (1). TJs seal cells to create a primary barrier to the diffusion of solutes across the cellular sheet and also function as a boundary between the apical and basolateral membrane domains to produce their polarization (2–5). Therefore, TJs are essential structures for epithelial cells to exert their physiological functions.

On ultrathin-section electron microscopy, TJs appear as a series of discrete sites of apparent fusion involving the outer leaflets of the plasma membranes of adjacent cells (1). On freeze-fracture electron microscopy, TJs appear as a set of continuous, anastomosing intramembranous particle strands (TJ strands) (6). TJ strands are mainly composed of linearly polymerized integral membrane proteins called claudins with molecular masses of ~23 kDa, which comprise a multigene family consisting of >20 members (5, 7, 8). Claudin molecules bear four transmembrane domains with both NH_2 and COOH termini located in the cytoplasm. In addition to claudins, two other types of integral membrane proteins have been reported to concentrate at TJs, occludin (9), and JAM (10).

One of the interesting questions regarding the molecular mechanism behind the morphogenesis of simple epithelial cells, *i.e.* epithelial polarization, is how claudins are polymerized exclusively at the most apical part of the junctional complex, *i.e.* more apically than AJs. In this connection, various scaffold proteins have been reported to be concentrated at the cytoplasmic surfaces of the junctional complex regions to determine the specialization and localization of junctions (5, 11, 12). At TJs, three closely related proteins called ZO-1, ZO-2, and ZO-3 were identified to constitute the plaque structures underlying plasma membranes (13, 14) together with various proteins including cingulin, symplekin, Par-3·Par-6·atypical protein kinase C complex, ZONAB, and guanine nucleotide exchange factor-H1/Lfc (15–19).

ZO-1 with a molecular mass of ~220 kDa was first identified as an antigen for a monoclonal antibody raised against a junction-enriched fraction from the liver (20). ZO-2 then was identified as a 160-kDa protein that was coimmunoprecipitated with ZO-1 from cell lysates (21). A phosphorylated 130-kDa protein was also found in the ZO-1 immunoprecipitate (22) and is now called ZO-3. The cloning and sequencing of cDNAs encoding these molecules showed that all have three PDZ domains (PDZ1–3), one Src homology 3 domain, and one guanylate kinase-like homologue domain in this order from their NH_2 termini, indicating that ZO-1, ZO-2, and ZO-3 are membrane-associated guanylate kinase-like homologues (MAGUKs) (23–26).

Among these three MAGUKs of TJs, ZO-1 is relatively well characterized. In well polarized epithelial cells, ZO-1 is exclu-

* This study was supported in part by a grant-in-aid for Cancer Research and a grant-in-aid for Scientific Research (A) from the Ministry of Education, Science and Culture of Japan (to S. T.). The costs of publication of this article were defrayed in part by the payment of page charges. This article must therefore be hereby marked "*advertisement*" in accordance with 18 U.S.C. Section 1734 solely to indicate this fact.

‖ To whom correspondence should be addressed: Dept. of Cell Biology, Faculty of Medicine, Kyoto University, Sakyo-ku, Kyoto 606-8501, Japan. Tel.: 81-75-753-4372; Fax: 81-75-753-4660; E-mail: htsukita@mfour.med.kyoto-u.ac.jp.

[1] The abbreviations used are: TJs, tight junctions; AJs, adherens junctions; JAM, junctional adhesion molecule; mAb, monoclonal antibody; pAb, polyclonal antibody; MAGUKs, membrane-associated guanylate kinase-like homologues; GST, glutathione *S*-transferase; PBS, phosphate-buffered saline; P_t, paracellular tracer flux; P_0, paracellular tracer flux at time 0; HA, hemagglutinin; TER, transepithelial electric resistance; FITC, fluorescein isothiocyanate.

sively concentrated at TJs through its direct binding to claudins (27), occludin (28, 29), and JAM (30, 31), whereas in non-epithelial cells lacking TJs such as fibroblasts and cardiac muscle cells as well as in epithelial cells at the initial phase of epithelial polarization, it is precisely colocalized with cadherins through direct and/or indirect interaction with α-catenin, a cadherin-associated protein (23). ZO-1 forms independent complexes with ZO-2 and ZO-3 (32) and binds to actin filaments at its COOH-terminal half (29, 33). These findings suggested that, together with ZO-2 (and ZO-3), ZO-1 plays a key role in the establishment of not only TJs but also AJs during epithelial polarization. To date, intensive efforts have been made to clarify the functions of ZO-1, for example, through exogenous expression of various deletion mutants of ZO-1 (29, 33, 34) but it has been difficult to experimentally dissect the physiological functions of ZO-1. Although there were no experimental data, this difficulty was thought to be partly due to a possible functional redundancy between ZO-1 and ZO-2 (and also ZO-3).

One of the most promising approaches to this problem would be to suppress the expression of endogenous ZO-1 in epithelial cells and to observe what happens in these cells. For this purpose, we attempted to apply the technology of RNA interference (35) to cultured mouse epithelial cells but failed to suppress the expression of ZO-1 completely. During the course of such RNA interference experiments, we noted that, to examine the functions of constituents of junctions in detail, the expression of each constituent should be "completely" and "stably" suppressed in cultured epithelial cells. In this study, we report that ZO-1-deficient mutants of cultured mouse epithelial cells were successfully generated by conventional homologous recombination and characterized in detail from the viewpoint of junction assembly. We believe that the gene knock-out at the level of cultured epithelial cells is important for a better understanding of the molecular mechanisms behind the junction formation and epithelial polarization.

EXPERIMENTAL PROCEDURES

Cells and Antibodies—Mouse Eph4 epithelial cells were grown in Dulbecco's modified Eagle's medium supplemented with 10% fetal calf serum. Eph4 cells were a gift from Dr. E. Reichman (Institute Suisse de Recherches, Lausanne, Switzerland) (36).

Mouse anti-ZO-1 mAb (T8–754) (23), rat anti-occludin mAb (MOC37), rat anti-ZO-3 mAb (37), and anti-JAM pAb (31) were raised and characterized previously. Rat anti-mouse E-cadherin mAb (ECCD2), rabbit anti-PAR-3/ASIP pAb, and rabbit anti-afadin pAb were provided by Dr. M. Takeichi (Center for Developmental Biology, Kobe, Japan), Dr. S. Ohno (Yokohama City University, Yokohama, Japan), and Dr. Y. Takai (Osaka University, Osaka, Japan), respectively. Rabbit anti-claudin-3 pAb, rabbit anti-ZO-2 pAb, and anti-HA mAb were purchased from Sigma, Santa Cruz Biotechnology, and Roche Applied Science, respectively. Rat anti-cingulin mAbs were generated using the GST fusion protein containing amino acids 216–419 of mouse cingulin as antigens.

Generation of ZO-1-deficient Eph4 Cells—A λ-phage 129/Sv mouse genomic library was screened using a mouse ZO-1 cDNA fragment as a probe. As shown in Fig. 1*A*, an 8.5-kb BstXI/NlaIV fragment and a 1.7-kb PvuII fragment were ligated to the targeting vector cassette. Gene targeting was performed twice to delete both alleles of the ZO-1 gene. The first and second targeting vectors contained a β-geo (β-galactosidase/neomycin-resistance gene) and hygromycin-resistance gene in the middle, respectively. For the first gene targeting, the targeting vector was linearized at a unique SacII site located at the 5′ end of the 5′-homologous fragment and then the trypsinized/floated Eph4 cells (2.0×10^7) were electroporated with 100 μg of linearized targeting vector DNA using a Gene Pulser (Bio-Rad). Cells were plated on six 10-cm dishes in Dulbecco's modified Eagle's medium supplemented with 10% fetal calf serum for 48 h and selected by adding G418 at a final concentration of 400 μg/ml. At day 14–17 of culture, the G418-resistant colonies were removed and screened by Southern blotting of EcoRI-digested DNA with the 3′-external probe. Correctly targeted clones were identified by a 8.6-kb band in addition to the 21-kb band of the wild-type allele. For the second gene targeting, the targeting vector was linearized at a unique XhoI site located at the 3′ end of the 3′-homologous fragment, and electroporation was performed as described above. Cells were cultured in the Dulbecco's modified Eagle's medium supplemented with 10% fetal calf serum for 48 h, and hygromycin and G418 were added at a final concentration of 300 μg/ml each. Colonies resistant to both hygromycin and G418 were screened by Southern blotting of EcoRI-digested DNA with the 3′-external probe, and correctly targeted clones were identified by a 9.0-kb band in addition to the 8.6-kb band of the first allele targeted.

Immunofluorescence Microscopy—Cells were cultured on Transwell filters 12 mm in diameter for 2 days. For ZO-1, ZO-2, Par-3, claudin-3, occludin, and E-cadherin staining, cells were fixed with 10% trichloroacetic acid for 30 min on ice (38). For afadin staining, cells were fixed with 2% paraformaldehyde in PBS for 10 min at room temperature. These cells were washed with PBS and then treated with 0.2% Triton X-100 in PBS for 10 min. For ZO-3, cingulin, and JAM staining, cells were fixed with 100% methanol for 3 min at −20 °C. After a wash with PBS, cells were soaked in 1% bovine serum albumin in PBS and incubated with the respective primary antibody for 1 h. Cells then were washed with PBS extensively and incubated with Alexa 488-conjugated (Molecular Probes) or Cy3-conjugated secondary antibody for 30 min (Jackson ImmunoResearch). They were washed with PBS and mounted in ProLong Antifader (Molecular Probes).

Ca^{2+} Switch—Cells were plated at 5×10^4 cells/well on Transwell filters 12 mm in diameter (Corning) and grown in the Dulbecco's modified Eagle's medium supplemented with 10% fetal calf serum for 48 h. They were then washed twice with PBS and cultured overnight in a low Ca^{2+} medium; S-MEM, calcium-free minimum Eagle's medium supplemented with 5 μM $CaCl_2$ and 10% fetal calf serum that had been pretreated with Chelex resin (Bio-Rad). For the Ca^{2+} switch, the low Ca^{2+} medium in both the upper and lower chambers was replaced with the normal Ca^{2+} medium (minimum Eagle's medium with 1.8 μM $CaCl_2$ and 10% fetal calf serum).

Measurement of Transepithelial Electric Resistance (TER) and Paracellular Tracer Flux—Aliquots of 5×10^4 cells were plated on Transwell filters 12 mm in diameter (8 filters for each cell line), and the culture medium was exchanged every day. After a 6-day culture, TER was measured directly in culture media using a Millicell-ERS epithelial voltohmmeter (Millipore). The TER values were calculated by subtracting the background TER of blank filters and by multiplying by the surface area of the filter.

For paracellular tracer flux assay, at 2, 6, 12, 24, 36, and 48 h after the Ca^{2+} switch, FITC-dextran with a molecular mass of 40 kDa was added to the medium in the apical compartment at a concentration of 2 mg/ml. After a 2-h incubation at each time point, a 100-μl aliquot of the medium was collected from the basal compartment and the paracellular tracer flux was measured as the amount of FITC-dextran in the medium with a fluorometer (P_t). The paracellular tracer flux at time 0 was measured without a Ca^{2+} switch in the low Ca^{2+} medium (P_0). "Permeability" was determined as the P_t/P_0 ratio.

Cell Aggregation Assay—Cells were plated on Transwell filters 24 mm in diameter (Corning) and grown overnight in the low Ca^{2+} medium. When incubated with Hepes-buffered saline (25 mM Hepes-NaOH, pH 7.2, 137 mM NaCl, 5 mM KCl, 0.7 mM Na_2HPO_4, and 6 mM dextrose) containing 5 mM EDTA at 37 °C for 30 min, most of the cells had detached from the filter as single cells. They then were centrifuged and resuspended in L-15 medium (normal Ca^{2+} concentration) (Invitrogen) supplemented with 10% fetal calf serum at a density of 1.5×10^6 cells/ml. Aliquots (0.5 ml) of this suspension were placed in 12-well non-tissue culture plates (FALCON). After 15-, 45-, 90-, or 180-min shaking on a gyratory shaker at 80 rpm to allow cell aggregation, the aggregates were enumerated with a hemocytometer. The extent of cell aggregation was represented by the index N_t/N_0, where N_t and N_0 are the total numbers of aggregates and cells per dish, respectively.

Immunoblotting and Quantitative Analysis of the ZO-1/ZO-2 Expression Levels—The SacII fragment of ZO-1 cDNA (7–143 amino acids) and the EcoRV fragment of ZO-2 cDNA (385–577 amino acids) were subcloned into the pGEX4T-1 and pGEX 4T-2 expression vectors, respectively. GST fusion proteins were expressed in *Escherichia coli* and purified using glutathione-Sepharose 4B beads (Amersham Biosciences) as previously described (28). The concentration of the GST fusion protein in each eluate was determined with a protein assay reagent (Bio-Rad) using bovine γ-globulin as a standard.

An appropriate amount of whole cell lysate and various amounts of GST-fused ZO-1 or ZO-2 were separated by SDS-PAGE on the same gel and immunoblotted with anti-ZO-1 mAb or anti-ZO-2 pAb, respectively, as described previously (28). We then compared the intensity of immu-

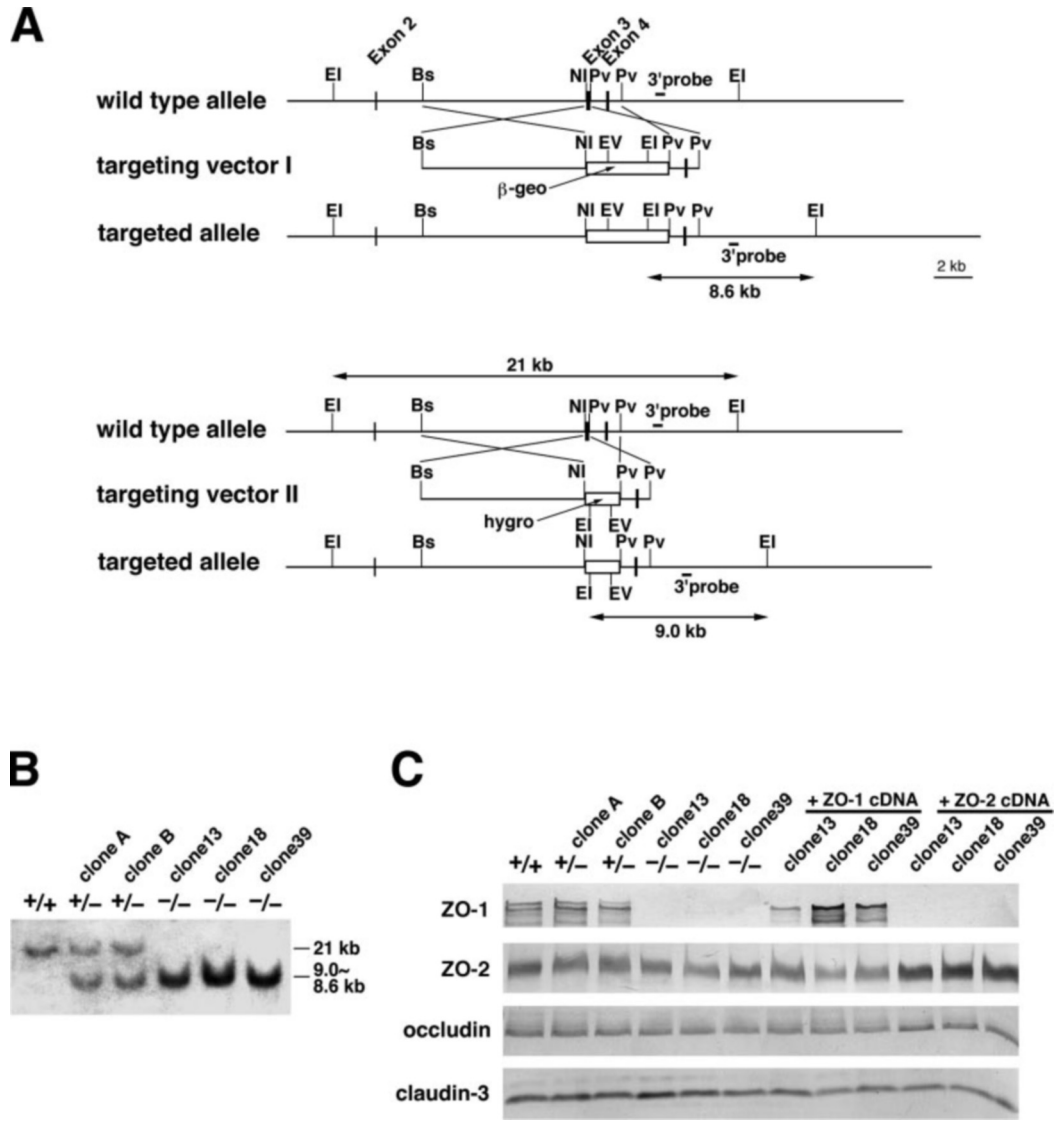

FIG. 1. **Generation of ZO-1-deficient Eph4 cells.** *A*, restriction maps of the wild-type allele, the first and second targeting vectors, and the targeted allele of the mouse ZO-1 gene. Putative exons 2–4 encoded most of the PDZ1 domain. The first and second targeting vectors contained a β-geo (β-galactosidase/neomycin-resistance gene) and hygromycin-resistance gene in the middle, respectively, to delete almost all of exon 3. The position of the 3′ probe for Southern blotting is indicated by *bars*. *EI*, EcoRI; *Bs*, BstXI; *Pv*, PvuII; *N1*, N1aIV. *B*, genotype analyses by Southern blotting of EcoRI-digested genomic DNA from wild-type (+/+), heterozygous (+/−; *clones A* and *B*), and homozygous (−/−; *clones 13*, *18*, and *39*) Eph4 cells. Southern blotting with the 3′ probe yielded a 21-kb band from the wild-type allele, a 8.6-kb band from the first targeted allele, and a 9.0-kb band from the second targeted allele (*A*). The 8.6- and 9.0-kb bands were not resolved into two bands. *C*, Western blotting of wild-type cell (+/+), *ZO-1*+/− cells (*clones A* and *B*), *ZO-1*−/− cells (*clones 13*, *18*, and *39*), *ZO-1*−/− cells exogenously expressing ZO-1 (+ZO-1 cDNA), and *ZO-1*−/− cells exogenously expressing HA-tagged ZO-2 (+ZO-2 cDNA). The whole cell lysates were immunoblotted with anti-ZO-1 mAb, anti-ZO-2 pAb, anti-occludin mAb, and anti-claudin-3 pAb. In *ZO-1*+/+ and ZO-1+/− cells, ZO-1 was detected as two bands, which corresponded to α(+) and α(−) isotypes. *ZO-1*−/− cells expressing the exogenous α(−) isotype of ZO-1 produced only one band.

noblotted bands of ZO-1 or ZO-2 in cell lysates with that of GST fusion proteins using Adobe Photoshop 7.0 histograms.

RESULTS

Homozygous Disruption of the ZO-1 Gene in Cultured Eph4 Epithelial Cells—To explore the function of ZO-1 in epithelial cells, we attempted to homozygously disrupt the ZO-1 gene in cultured epithelial cells. In an attempt to share the same targeting vectors for the gene knock-out analyses between the cultured cell and whole body levels in mice, we searched for appropriate "mouse" epithelial cell lines for gene targeting. Based on the stability of the well polarized epithelial morphology as well as the growth rate, we eventually chose the Eph4 cell line originally established from mouse mammary glands (36).

The genomic structure of the mouse ZO-1 gene was partially clarified as shown in Fig. 1*A*. Putative exons 2–4 encoded most of the PDZ1 domain. Two targeting vectors were constructed with the expectation that homologous recombination between the vectors and the ZO-1 gene would result in a deletion of almost all (125 bp) of exon 3 (Fig. 1*A*). In the first targeting and screening, the wild-type ZO-1 allele displayed a 21-kb band on Southern blotting of EcoRI-digested DNA with the 3′ probe, whereas the disrupted locus showed an 8.6-kb band (Fig. 1*B*). Of the 96 G418-resistant clones examined, 5 independent clones had undergone a single homologous recombination event.

Two of these five clones (Fig. 1*B*, *clones A* and *B*) then were expanded and subjected to the second targeting. When the wild-type allele was targeted by the second vector, Southern blotting of EcoRI-digested DNA with the 3′ probe was expected to generate a 9.0-kb band (Fig. 1*A*). As shown in Fig. 1*B*, 1 of 68 hygromycin-resistant clones derived from clone A (clone 13)

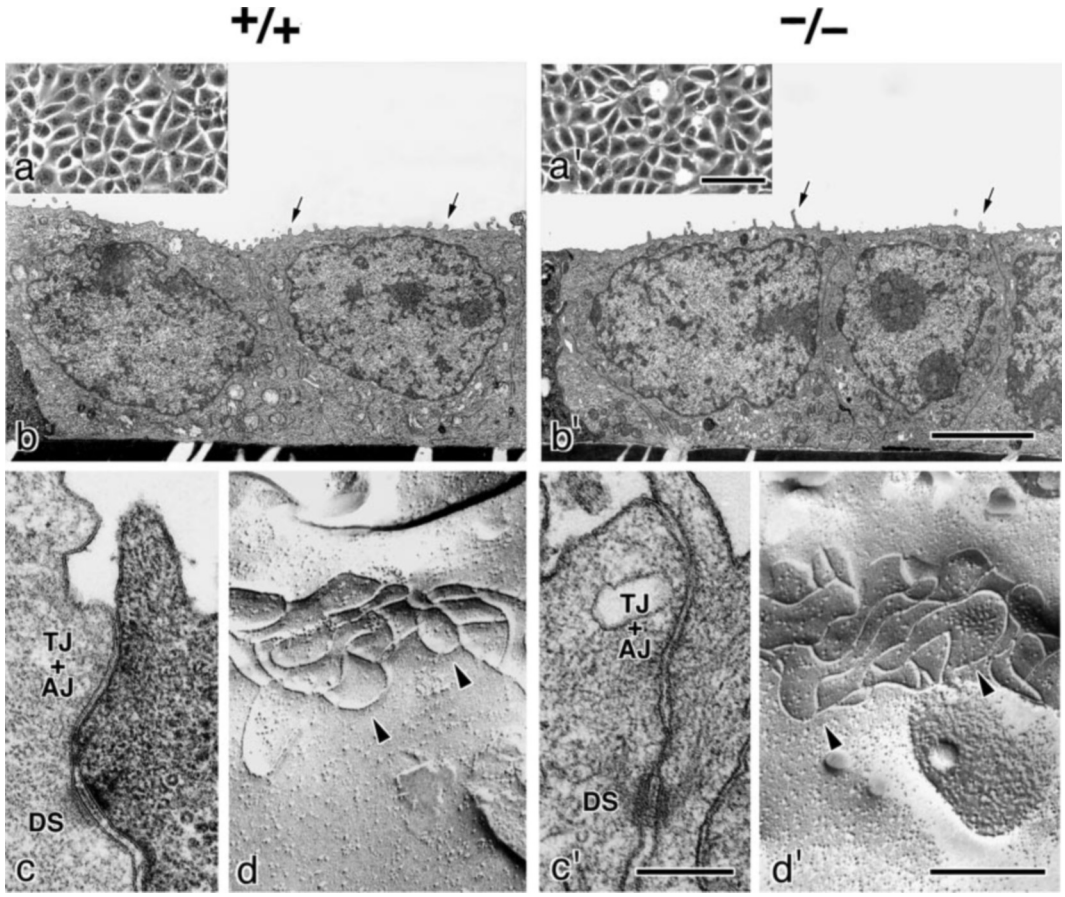

FIG. 2. **Morphology of *ZO-1*+/+ and *ZO-1*−/− Eph4 cells cultured under highly confluent conditions.** *a* and *a′*, phase-contrast microscopy. *ZO-1*+/+ and ZO-1−/− cells showed a cobble stone-like appearance. *b* and *b′* and *c* and *c′*, ultrathin-section electron microscopy. Both *ZO-1*+/+ and *ZO-1*−/− cells were highly polarized. They bore short microvilli on their apical surface (*arrows*, *b* and *b′*) and a well organized junctional complex in the most apical region of lateral membranes (*c* and *c′*). In Eph4 cells, TJs were not clearly segregated from AJs (*TJ*+*AJ*). *DS*, desmosome. *d* and *d′*, freeze-fracture replica electron microscopy. TJs of *ZO-1*+/+ cells were characterized by a well developed network of P-face-associated TJ strands (*arrowheads*), and ZO-1 deficiency did not alter these characteristics. Electron microscopy was performed as described previously (49). *Bars*, 20 μm (*a* and *a′*); 4 μm (*b* and *b′*); 300 nm (*c* and *c′*); and 300 nm (*d* and *d′*).

and two of 97 hygromycin-resistant clones derived from clone B (clone 18 and 39) lacked the wild-type 21-kb band and instead showed ~9-kb thick bands in which the 8.6- and 9.0-kb bands might not be resolved. Correct targeting in clones A/B/13/18/39 was confirmed by Southern blotting with a 5′ probe, and targeted clones were also checked for single integration by hybridization with a β-galactosidase or hygromycin resistance gene probe (data not shown).

We next confirmed the loss of ZO-1 expression in clones 13, 18, and 39 at the protein level. We performed immunoblotting analyses using an anti-ZO-1 mAb that recognizes both the α(+) and α(−) isotypes of ZO-1. As shown in Fig. 1*C*, both isotypes were detected in the wild-type as well as two *ZO-1*+/− clones (*clones A* and *B*), but in clones 13, 18, and 39, no trace of either ZO-1 isotype was detectable, even when their cell lysates were overloaded.

Furthermore, we introduced cDNA encoding the α(−) isotype of ZO-1 or HA-tagged ZO-2 into clones 13, 18, and 39 and obtained stable transfectants. Their expression was confirmed by immunoblotting (Fig. 1*C*). Because clones 13, 18, and 39 showed the same phenotype as far as was examined, the data obtained from clone 18 (and the clone 18 transfectant expressing exogenous ZO-1 and HA-ZO-2) are mostly represented below.

Morphology, Growth, and Motility of ZO-1-deficient Eph4 Cells—We cultured ZO-1-deficient Eph4 cells (*ZO-1*−/− cells; clone 18) on a coverslip under confluent conditions. Phase-contrast microscopy revealed that these cells appeared to completely retain the epithelial morphology. They showed a typical cobble stonelike appearance (Fig. 2, *a* and *a′*). No significant difference was discerned between wild-type (*ZO-1*+/+) and *ZO-1*−/− Eph4 cells in the size of individual cells and the appearance of the cell-cell contacts. Also at the ultrathin-section electron microscopic level, *ZO-1*−/− cells were indistinguishable from *ZO-1*+/+ cells. They appeared to be well polarized with apical membranes bearing characteristic short microvilli (Fig. 2, *b* and *b′*). In good agreement, preliminary observations indicated that immunofluorescence staining patterns with "apical" markers did not appear to change between *ZO-1*+/+ and *ZO-1*−/− cells (data not shown). The appearance of the junctional complex did not appear to be altered by the deficiency of *ZO-1*, although it was difficult to clearly distinguish TJs from AJs both in *ZO-1*+/+ and in *ZO-1*−/− cells using ultrathin sectional images (Fig. 2, *c* and *c′*). We then compared the morphology of TJs of *ZO-1*−/− cells and *ZO-1*+/+ cells by freeze-fracture replica electron microscopy. As shown in Fig. 2*d*, the TJs of *ZO-1*+/+ cells were characterized by a well developed network of "P-face-associated" intramembranous particle strands and the lack of ZO-1 did not alter these characteristics (Fig. 2, *d* and *d′*).

We next compared the growth rate and motility of *ZO-1*−/− cells with those of *ZO-1*+/+ cells. As shown in Fig. 3*A*, simple cell counting revealed that *ZO-1*−/− cells had the same growth curve as *ZO-1*+/+ cells. Furthermore, the wound-healing assay with the confluent cultures showed that *ZO-1*−/− cells moved

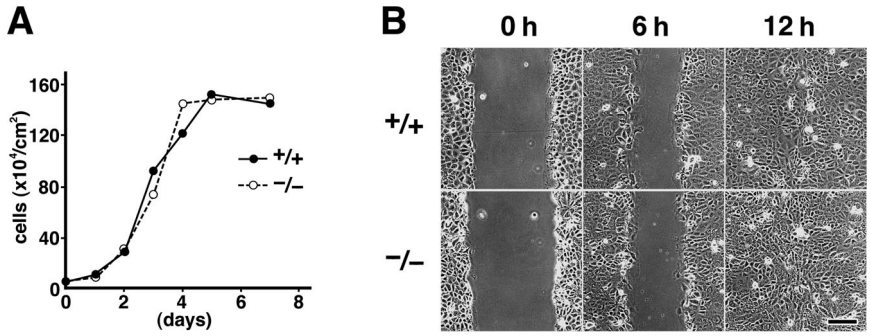

FIG. 3. **Growth and motility of *ZO-1*−/− Eph4 cells.** *A*, cell growth curve. *ZO-1*+/+ and ZO-1−/− cells were plated on Transwell filters 12 mm in diameter at 5×10^4 cells/well. At 1, 2, 3, 4, 5, and 7 days, cells were dissociated into single cells by treatment with 0.25% trypsin at 37 °C for 10 min. Cell growth was measured by making duplicate counts of these cells with a hemocytometer. Note that *ZO-1*+/+ and *ZO-1*−/− cells grew with the same time course. *B*, wound healing assay. Confluent cultures of well polarized *ZO-1*+/+ and *ZO-1*−/− cells (1×10^6 cells/dish) were manually scratched with a pipette tip. The linear regions were allowed to heal for 12 h and were observed by phase-contrast microscopy. ZO-1+/+ and ZO−/− cells moved toward the wounded region at the same rate. *Bar*, 50 μm.

toward the wounded region as quickly as *ZO-1*+/+ cells (Fig. 3*B*).

Molecular Assembly of TJs in ZO-1-deficient Eph4 Cells—In confluent cultures, *ZO-1*−/− cells were well polarized and formed the TJs of normal appearance. We then examined the molecular assembly of TJs in these cells by immunofluorescence microscopy. As controls, we used *ZO-1*+/+ and *ZO-1*−/− cells (clone 18) exogenously expressing the α(−) isotype of *ZO-1* (*ZO-1*−/−/+ cells). First, cells were cultured on Transwell filters under highly confluent conditions ($2–3 \times 10^5$ cells/cm^2) and immunofluorescently stained with antibodies specific for the components of the plaque structures of TJs (Fig. 4*A*). Of course, ZO-1 was undetectable at TJs of *ZO-1*−/− cells and the concentration of ZO-1 at TJs in *ZO-1*−/−/+ cells appeared to be comparable with that in *ZO-1*+/+ cells. Interestingly, the ZO-2 signal was significantly increased at TJs in *ZO-1*−/− cells as compared with *ZO-1*+/+ cells and this increase of the ZO-2 signal at TJs was suppressed to the *ZO-1*+/+ cell level by exogenous expression of ZO-1. ZO-3 was undetectable in parental *ZO-1*+/+ cells by immunofluorescence microscopy, which was consistent with our previous study (37). ZO-3 did not become detectable in *ZO-1*−/− cells. Among non-MAGUK components of the TJ plaque structure, cingulin was clearly affected in its distribution in *ZO-1*−/− cells. Cingulin became undetectable from TJs in *ZO-1*−/− cells but was clearly recovered at TJs in *ZO-1*−/−/+ cells. In *ZO-1*−/− cells, no significant changes were observed in the subcellular distribution of other TJ plaque components such as Par-3 (Fig. 4*A*) and Par-6 (data not shown), for example.

We next examined the behavior of TJ integral membrane proteins, claudins, occludin, and JAM, in *ZO-1*−/− cells (Fig. 4*B*). At least four distinct species of claudins, claudin-1, -3, -4, and -7, were expressed in parental *ZO-1*+/+ cells. As these four claudins behaved in the same way in all of the experiments and as the combination of expressed claudins did not appear to be changed by ZO-1 deficiency, the behavior of claudin-3 is presented as being representative in this study. Under highly confluent conditions, claudin-3, occludin, and JAM were clearly concentrated at TJs in *ZO-1*−/− cells, showing no significant differences in the distribution and concentration at TJs as compared with *ZO-1*+/+ and *ZO-1*−/−/+ cells. In *ZO-1*−/− cells, the distribution of AJ-related proteins such as E-cadherin and afadin also appeared to be normal (Fig. 4*B*) and the organization of phalloidin-positive actin-based cytoskeletons did not appear to be affected (Fig. 4*C*).

In terms of the molecular architecture of TJs and AJs, clear alterations were detected in ZO-2 and cingulin was detected in *ZO-1*−/− cells. We then compared the behavior of ZO-2 more precisely among various Eph4 clones by the method of mixed culture. *ZO-1*+/+ cells were mixed and cocultured with *ZO-1*−/− cells and then subjected to double immunofluorescence staining with anti-ZO-1 mAb and anti-ZO-2 pAb (Fig. 5*a*). As described above, the ZO-2 signal from TJs became more intense in *ZO-1*−/− cells than in *ZO-1*+/+ cells. Interestingly, in *ZO-1*−/− cells, the ZO-2 signal from the cytoplasm was significantly decreased as compared with *ZO-1*+/+ cells. These findings suggested that the ZO-1 deficiency biased the distribution of ZO-2 from the cytoplasm to TJs in *ZO-1*−/− cells. The mixed culture of *ZO-1*−/− and *ZO-1*−/−/+ cells revealed that this TJ-biased localization of ZO-2 was abolished with the exogenous expression of ZO-1 (Fig. 5*b*).

We next undertook a detailed examination of the behavior of cingulin. As noted above, cingulin disappeared from TJs in *ZO-1*−/− cells and the phenotype was completely rescued by exogenous expression of ZO-1 (see Fig. 4*A*). Interestingly, this rescue was not achieved by the exogenous overexpression of HA-ZO-2, indicating that, in terms of the recruitment of cingulin to TJs, ZO-2 was not functionally redundant for ZO-1 (Fig. 6*A*). These findings were confirmed using two independent anti-cingulin mAbs. Northern and Western blotting revealed that, in *ZO-1*−/− cells, either the expression level of mRNA or of protein of cingulin was not down-regulated, indicating that the ZO-1 deficiency simply affected the recruitment of cingulin to TJs (Fig. 6, *B* and *C*).

Formation of Tight and Adherens Junctions in ZO-1-deficient Eph4 Cells—We next compared the process of junction formation, *i.e.* epithelial polarization among *ZO-1*+/+, ZO-1−/−, and ZO-1−/−/+ cells. For this purpose, the cells were cultured in a low Ca^{2+} medium containing 5 μM Ca^{2+} overnight under confluent conditions and then their polarization was initiated by transferring them to a normal Ca^{2+} medium. The degree of TJ formation first was evaluated by immunofluorescence staining with anti-claudin-3 pAb or anti-occludin mAb. As shown in Fig. 7, *ZO-1*+/+ cells began to form continuous claudin-3/occludin-positive TJs at 2 h and appeared to have mostly completed the process at 4 h after being transferred to the normal Ca^{2+} medium. By contrast, in the *ZO-1*−/− cell sheets, even after a 10-h incubation in the normal Ca^{2+} medium, the claudin-3/occludin-positive TJs were still fragmentary. This discontinuity of TJs in *ZO-1*−/− cells was decreased by further culture in the normal Ca^{2+} medium nearly down to the *ZO-1*+/+ cell level. This ZO-1 deficiency-induced retardation of TJ formation was completely rescued by exogenous expression of ZO-1 (see −/− + *ZO-1 cDNA* in Fig. 7). Interestingly, when the TJ formation was evaluated by immunostaining with anti-ZO-2 pAb, at 2 h after the Ca^{2+} switch, endogenous ZO-2 was concentrated rather weakly along continuous TJs in *ZO-1*+/+ cells,

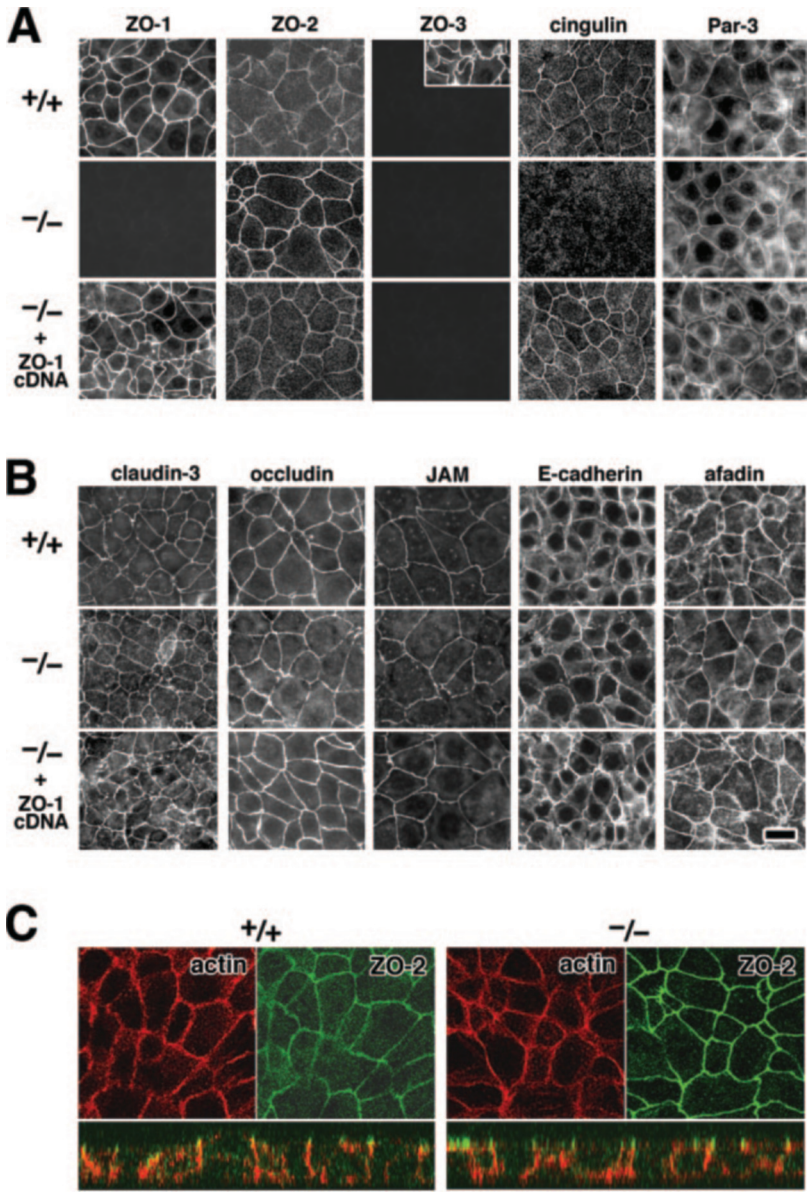

FIG. 4. **Molecular assembly of junctions in *ZO-1*−/− Eph4 cells.** *ZO-1*+/+ cells (+/+), *ZO-1*−/− cells (−/−), and *ZO-1*−/− cells exogenously expressing the α(−) isotype of ZO-1 (−/− + *ZO-1 cDNA*) were cultured on Transwell filters under highly confluent conditions and immunofluorescently stained with antibodies specific for the components of the plaque structures of TJs (*A*), TJ integral membrane proteins, claudin-3, occludin and JAM (*B*), the constituents of AJs, E-cadherin and afadin (*B*), or actin filaments (rhodamine-conjugated phalloidin) (*C*). ZO-1 deficiency was confirmed in *ZO-1*−/− cells. ZO-2 appeared to be accumulated at TJs in *ZO-1*−/− cells, and this increase was abolished with the expression of exogenous ZO-1. ZO-3 was undetectable in all of these cells (*inset*, ZO-3 staining in another type of cultured mouse epithelial cell, MTD-1A). Cingulin disappeared from TJs in *ZO-1*−/− cells and was recovered to the wild-type level on exogenous expression of ZO-1. The distribution of other components of TJs and AJs as well as actin filaments did not appear to be affected by the ZO-1 deficiency. In *C*, images were acquired from cells double-stained with rhodamine-conjugated phalloidin (*red*) and anti-ZO-2 pAb (*green*) by confocal microscopy, and their cross-sectional images (*lower panels*) were computer-generated. *Bar*, 10 μm.

whereas in *ZO-1*−/− cells, ZO-2 signals from junctions were very intense but fragmentary, showing a pattern similar to that of claudin-3/occludin staining.

The process of TJ formation was then quantitatively evaluated. First, we compared the TER values among *ZO-1*+/+, ZO-1−/−, and ZO-1−/−/+ cells under highly confluent conditions. As shown in Fig. 8*A*, there was no significant difference detected in these values. However, Eph4 cells exhibited fairly low TER values (100–200 ohms cm^2), which were much lower than MDCK-I cells (~10,000 ohms cm^2), and these TER values varied widely depending on culture conditions. Therefore, it was difficult to evaluate the process of TJ formation after the Ca^{2+} switch by measuring TER values. Instead, we performed the paracellular tracer flux assay. *ZO-1*+/+, ZO-1−/−, or ZO-1−/−/+ cells were cultured on Transwell filters in the low Ca^{2+} medium at a confluent density, and then epithelial polarization was initiated by changing the medium in both the apical and basal compartments from a low to normal Ca^{2+} concentration. At 2, 6, 12, 24, 36, and 48 h after the Ca^{2+} switch, FITC-dextran with a molecular mass of 40 kDa then was added to the medium in the apical compartment. After a 2-h incubation at each time point, the medium in the basal compartment was collected and the paracellular tracer flux was determined as the amount of FITC-dextran in the medium measured with a fluorometer. As shown in Fig. 8*A*, after the Ca^{2+} switch, the establishment of paracellular sealing was significantly delayed in *ZO-1*−/− cell sheets as compared with *ZO-1*+/+ and ZO-1−/−/+ cell sheets; however, interestingly, at around 48 h of incubation in the normal Ca^{2+} medium, the paracellular tracer flux of *ZO-1*−/− cell sheets reached almost the same level as that of ZO-1+/+ and ZO-1−/−/+ cell sheets.

The next question is whether this retardation of TJ formation in *ZO-1*−/− cells can be rescued by exogenous overexpression of ZO-2. In terms of the paracellular flux, exogenous overexpression of ZO-2 did not rescue the ZO-1 deficiency (Fig. 8*A*). The process by which TJs form in *ZO-1*−/− cells exogenously expressing HA-ZO-2 then was compared with that in *ZO-1*−/− and ZO-1−/−/+ cells by immunofluorescence microscopy. As shown in Fig. 8*B*, exogenous ZO-1 expression clearly promoted the process of TJ formation, *i.e.* recruitment of occludin and claudin-3 to cell-cell borders, in *ZO-1*−/− cells up to the normal level, whereas exogenous ZO-2 expression had no effect, indicating that, in the promotion of TJ formation, ZO-2 was not functionally redundant.

Finally, using the same Ca^{2+} switch method, the degree of AJ formation was evaluated by immunofluorescence staining

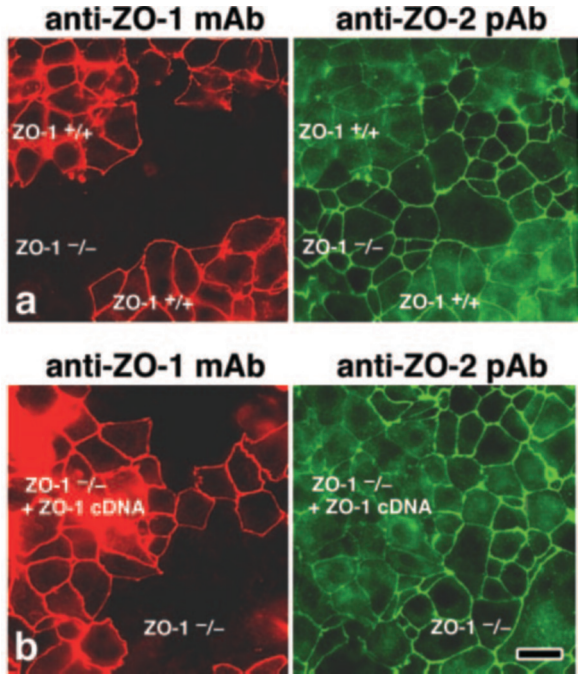

FIG. 5. **Effects of ZO-1 deficiency on ZO-2.** *a*, *ZO-1*+/+ cells were mixed and cocultured with *ZO-1*−/− cells and double stained with anti-ZO-1 mAb and anti-ZO-2 pAb. In *ZO-1*+/+ cells, significant amounts of ZO-2 were detected in the cytoplasm in addition to relatively weak ZO-2 staining at TJs, whereas in *ZO-1*−/− cells, ZO-2 appeared to be recruited from the cytoplasm to TJs, resulting in a decrease and increase in the amount of ZO-2 in the cytoplasm and TJs, respectively. *b*, the mixed culture of *ZO-1*−/− cells and *ZO-1*−/− cells expressing ZO-1 (*ZO-1*−/− + ZO-1 cDNA) revealed that the exogenous expression of ZO-1 recovered the distribution of ZO-2 in the cytoplasm. *Bars*, 10 μm.

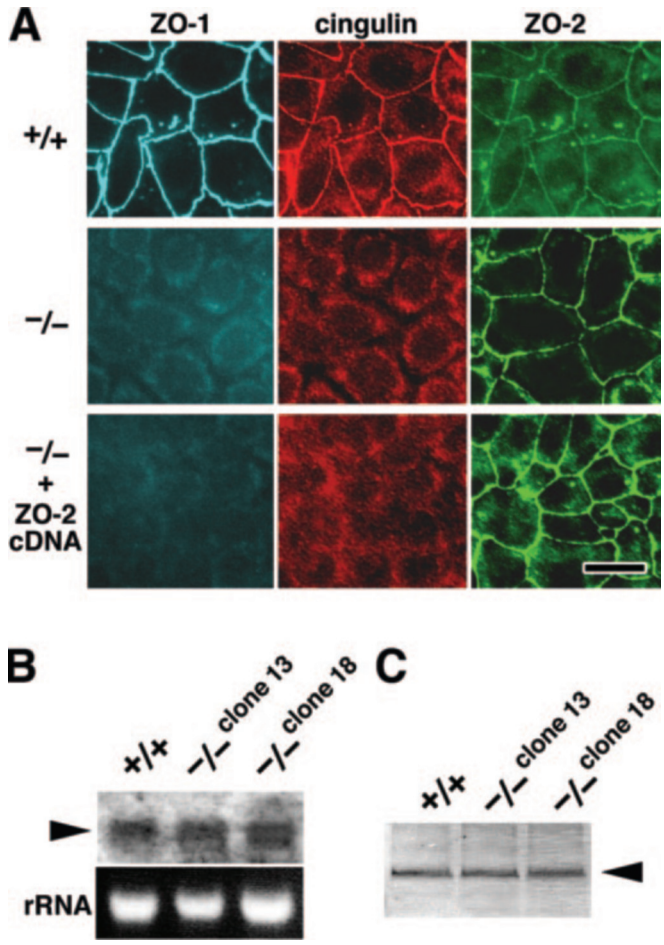

FIG. 6. **Effects of ZO-1 deficiency on cingulin.** *A*, *ZO-1*+/+ cells (+/+), *ZO-1*−/− cells (−/−), and *ZO-1*−/− cells exogenously expressing HA-ZO-2 (−/− + *ZO-2 cDNA*) were cultured on Transwell filters under highly confluent conditions and then immunofluorescently triple-stained with mouse anti-ZO-1 mAb, rat anti-cingulin mAb, and rabbit anti-ZO-2 pAb. At TJs of *ZO-1*−/− cells, cingulin disappeared, whereas the ZO-2 signal was increased. When HA-ZO-2 was overexpressed in *ZO-1*−/− cells, cingulin was still undetectable at TJs. *Bar*, 10 μm. *B*, Northern blotting. Total RNA was isolated from cells according to the TRIzol method (Invitrogen) and hybridized with digoxigenin-labeled DNA probes. In *ZO-1*−/− cells (−/− *clones 13* and *18*), the mRNA expression of cingulin (*arrowhead*) was not down-regulated as compared with *ZO-1*+/+ cells (+/+). *B*, Western blot analysis of the whole cell lysate of *ZO-1*+/+ (+/+) and *ZO-1*−/− cells (−/− *clones 13* and *18*) with anti-cingulin mAb. An equal amount of cell lysate was applied in each lane. Note that there is no significant difference in the amount of cingulin (*arrowhead*) between *ZO-1*+/+ and *ZO-1*−/− cells.

with anti-E-cadherin pAb (Fig. 9*A*). In contrast to TJ formation, AJ formation, *i.e.* the linear concentration of E-cadherin at cell-cell borders, did not appear to be affected by ZO-1 deficiency. Just after the Ca^{2+} switch, in *ZO-1*−/− cells, E-cadherin was quickly recruited to cell-cell contacts over a similar time course to *ZO-1*+/+ and ZO-1−/−/+ cells. Consistently, the cell aggregation assay quantitatively revealed that E-cadherin-based cell-cell adhesion activity was not affected by ZO-1 deficiency and that the activation of E-cadherin was induced with a normal time course in *ZO-1*−/− cells by the Ca^{2+} switch (Fig. 9*B*).

Expression Levels of ZO-1 and ZO-2 in Various Eph4 Clones—To interpret the present data precisely, the expression levels of ZO-1 and ZO-2 were examined in detail at both the mRNA and protein levels. Northern blotting revealed that, in *ZO-1*−/− cells (clones 13 and 18), the expression of ZO-2 mRNA was not up-regulated compared with that in parental *ZO-1*+/+ cells (Fig. 10*A*). In good agreement with the immunofluorescence observation (see Fig. 4*A*), ZO-3 was undetectable or detected only in a trace amount by Northern blotting not only in *ZO-1*+/+ cells but also in *ZO-1*−/− cells (data not shown), indicating that, in this Eph4 cell system, there is no need to take ZO-3 into consideration when discussing the possible functional redundancy among TJ MAGUKs.

We then quantitatively examined the expression levels of ZO-1 and ZO-2 in four distinct Eph4 clones: *ZO-1*+/+ cells; *ZO-1*−/− cells (clone 18); *ZO-1*−/−/+ cells; and *ZO-1*−/− cells expressing HA-ZO-2 (Fig. 10*B* and Table I). For this purpose, we first produced GST fusion proteins with a part of ZO-1 and ZO-2 in *E. coli* (see details in "Experimental Procedures") and purified them. We then compared the intensity of immunoblotted ZO-1 and ZO-2 in cell lysates with that of immunoblotted bands of various amounts of purified respective GST fusion proteins. In parental *ZO-1*+/+ cells, endogenous ZO-1 and ZO-2 concentrations were determined, respectively, to be 13.0 ± 1.0 and 8.2 ± 0.1 nmol/1 g total protein (mean ± S.E.). In *ZO-1*−/− cells, the amount of ZO-2 was not increased (9.4 ± 0.7 nmol/g), and in *ZO-1*−/−/+ cells, ZO-1 was overexpressed to some extent at 34.5 ± 4.5 nmol/g. Importantly, in *ZO-1*−/− cells expressing HA-ZO-2, the total amount of endogenous ZO-2 and HA-ZO-2 was estimated to be 19.8 ± 0.7 nmol/g, which was comparable with the total amount of endogenous ZO-1 and ZO-2 in *ZO-1*+/+ cells (~21 nmol/g) (Table I).

DISCUSSION

During the formation of junctions in simple epithelial cells, ZO-1 behaves in a very peculiar way. In the initial phase of the process, ZO-1 is colocalized with cadherins (and nectins) in primordial spotlike AJs at the tips of cellular protrusions (39–41). These ZO-1-positive spotlike AJs gradually fuse to form

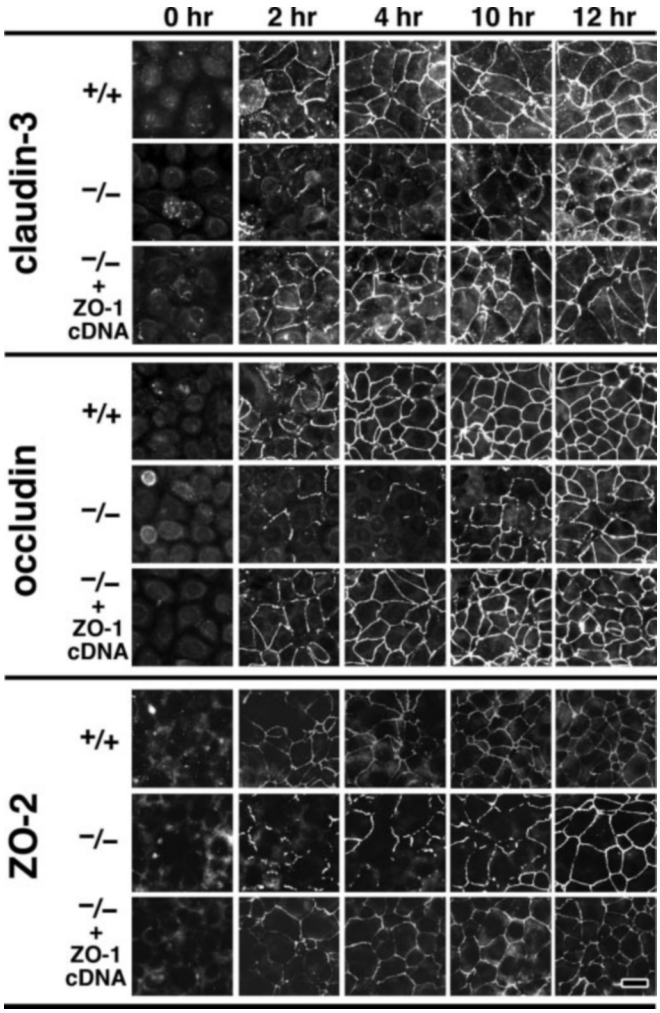

FIG. 7. **Retardation of the recruitment of claudin-3, occludin and ZO-2 to junctional areas in *ZO-1*−/− cells during epithelial polarization.** *ZO-1*+/+ cells (+/+), *ZO-1*−/− cells (−/−), and *ZO-1*−/− cells exogenously expressing ZO-1 (−/− + ZO-1 cDNA) were cultured in the low Ca^{2+} medium containing 5 μM Ca^{2+} overnight under confluent conditions, and then their polarization was initiated by transferring them to a normal Ca^{2+} medium. At a 0-, 2-, 4-, 10-, or 12-h incubation, cells were immunofluorescently stained with anti-claudin-3 pAb, anti-occludin mAb, or anti-ZO-2 pAb. The recruitment of claudin-3, occludin, and ZO-2 was significantly retarded in *ZO-1*−/− cells as compared with *ZO-1*+/+ cells, and this retardation was canceled by the exogenous expression of ZO-1. *Bars*, 10 μm.

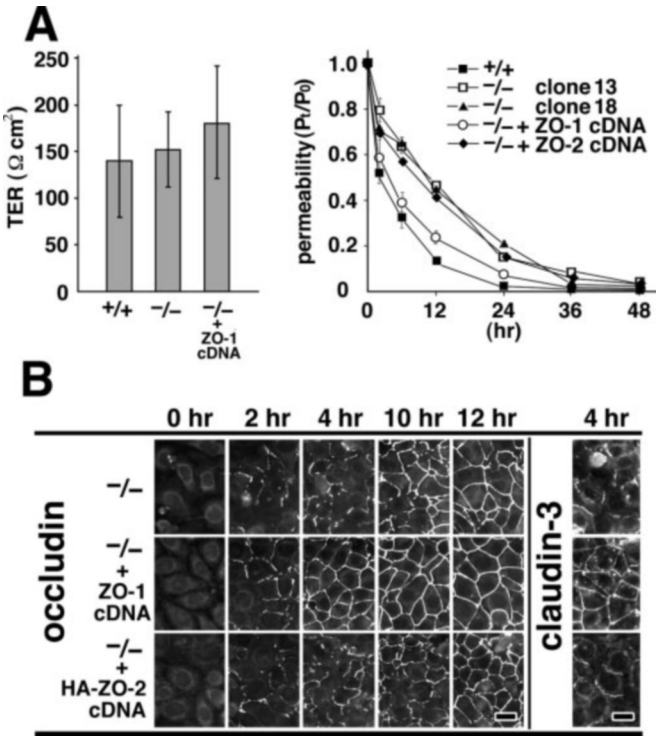

FIG. 8. **Retardation of TJ formation in *ZO-1*−/− cells during epithelial polarization.** *A*, TER measurements (*left*) and paracellular tracer flux assay (*right*). When the TER values were compared among *ZO-1*+/+, *ZO-1*−/−, and *ZO-1*−/−/+ cells under highly confluent conditions (see "Experimental Procedures"), there was no significant difference detected. However, Eph4 cells exhibited fairly low TER values (100–200 ohm cm^2) and these TER values varied widely depending on culture conditions. Therefore, it was difficult to evaluate the process of TJ formation after the Ca^{2+} switch by measuring TER values. Instead, we performed the paracellular tracer flux assay. *ZO-1*+/+ cells, two clones of *ZO-1*−/− cells (*clones 13* and *18*), *ZO-1*−/− cells exogenously expressing ZO-1 (*−/− + ZO-1 cDNA*) and *ZO-1*−/− cells exogenously expressing HA-tagged ZO-2 (*−/− + ZO-2 cDNA*) were cultured on Transwell filters in a low Ca^{2+} medium containing 5 μM Ca^{2+} overnight under confluent conditions, and then epithelial polarization was initiated by changing both the apical and basal compartment media from the low to normal Ca^{2+} concentrations. At 2, 6, 12, 24, 36, and 48 h after the Ca^{2+} switch, FITC-dextran with a molecular mass of 40 kDa was added to the apical compartment. After a 2-h incubation at each time point, the medium in the basal compartment was collected and the paracellular tracer flux was measured as the amount of FITC-dextran in the medium with a fluorometer (P_t). The paracellular tracer flux at time 0 was measured without a Ca^{2+} switch in the low Ca^{2+} medium (P_0). Permeability was determined as the P_t/P_0 ratio. Note that the establishment of a TJ barrier was clearly retarded in *ZO-1*−/− cells and that this retardation was canceled by the exogenous expression of ZO-1. *B*, effects of overexpression of HA-ZO-2 on the retardation of TJ formation. The recruitment of occludin (and claudin-3) to junctional areas in *ZO-1*−/− cells expressing HA-tagged ZO-2 (*−/− + HA-ZO-2 cDNA*) was compared with that in *ZO-1*−/− cells and *ZO-1*−/− cells exogenously expressing ZO-1 (*−/− + ZO-1 cDNA*). Exogenous ZO-2 did not compensate for the ZO-1 deficiency in terms of TJ formation. *Bar*, 10 μm.

beltlike junctions, at which time claudins/occludin begin to be recruited to these junctional areas to be polymerized as TJ strands (42). Interestingly, when TJs are finally segregated from AJs in well polarized epithelial cells, ZO-1 is completely excluded from AJs to be concentrated specifically at TJs (20, 23). These observations have led us to speculate that ZO-1 plays a crucial role in the formation of AJs and/or TJs as well as the epithelial polarization. Therefore, it was a big surprise to us when we found that, under confluent conditions, Eph4 cells specifically lacking the expression of ZO-1 (*ZO-1*−/− cells) were highly polarized with well organized junctional complexes even at the ultrathin and freeze-fracture replica electron microscopic levels. Furthermore, taking previous studies on ZO-1 into consideration (14, 17, 19), it was also unexpected that *ZO-1*−/− cells did not show any significant abnormality in their growth and motility.

However, close analyses revealed that *ZO-1*−/− cells showed three characteristic features distinct from parental Eph4 cells (*ZO-1*+/+ cells). First, immunofluorescent labeling of ZO-2 was markedly increased at TJs of *ZO-1*−/− cells. In *ZO-1*−/− cells, mRNA or protein expression of ZO-2 was not up-regulated and coculture experiments clearly revealed that the ZO-2 signal from the cytoplasm was significantly decreased in *ZO-1*−/− cells. Therefore, we concluded that the ZO-1 deficiency biased the distribution of ZO-2 from cytoplasm to TJs, not simply exploring more binding sites for anti-ZO-2 pAb at TJs. This finding clearly showed that ZO-2 can target to TJs without forming a complex with ZO-1 (32). It has been thought that the cytoplasmic surface of individual TJ strands (claudin polymers) appears as a toothbrush consisting of numerous short and densely packed COOH-terminal cytoplasmic tails of claudins,

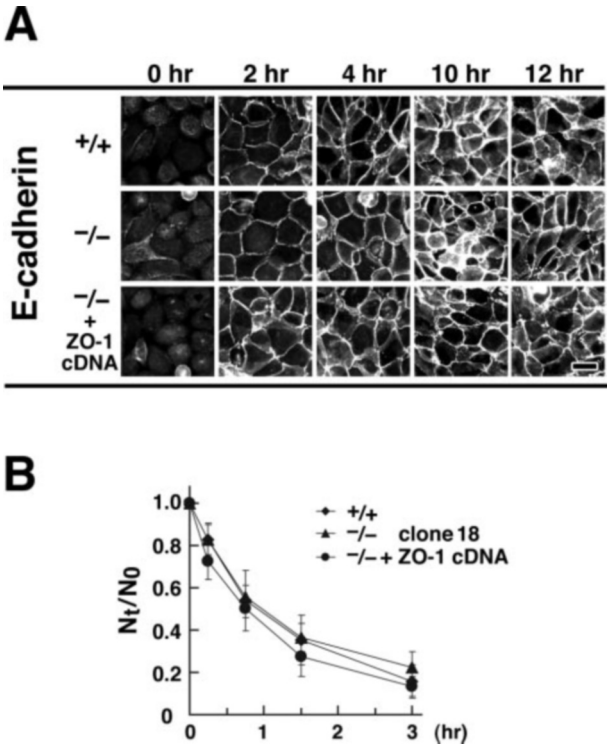

FIG. 9. **AJ formation in *ZO-1*−/− cells during epithelial polarization.** *A*, recruitment of E-cadherin to cell-cell contact sites. *ZO-1*+/+ cells (+/+), *ZO-1*−/− cells (−/−), and *ZO-1*−/− cells exogenously expressing ZO-1 (−/− + ZO-1 cDNA) were cultured in a low Ca^{2+} medium containing 5 μM Ca^{2+} overnight under confluent conditions, and then their polarization was initiated by transferring them to a normal Ca^{2+} medium. At a 0-, 2-, 4-, 10-, or 12-h incubation, cells were immunofluorescently stained with anti-E-cadherin pAb. The recruitment of E-cadherin appeared to be normal in *ZO-1*−/− cells. E-cadherin has already concentrated at AJs continuously in a linear fashion at 2 h after the Ca^{2+} switch. Bar, 10 μm. *B*, cell aggregation assay. *ZO-1*+/+ cells (+/+), *ZO-1*−/− cells (−/−; *clone 18*), and *ZO-1*−/− cells exogenously expressing ZO-1 (−/− + *ZO-1 cDNA*) were dissociated into single cells in a low Ca^{2+} medium containing 5 μM Ca^{2+} (see "Experimental Procedures") and were transferred to a normal Ca^{2+} medium. After a 15-, 45-, 90-, or 180-min shaking on a gyratory shaker at 80 rpm to allow cell aggregation, the aggregates were enumerated with a hemocytometer. The extent of cell aggregation was represented by the index N_t/N_0, where N_t and N_0 are the total numbers of aggregates and cells per dish, respectively. Note that ZO-1 deficiency did not affect the cadherin-based cell aggregation activity.

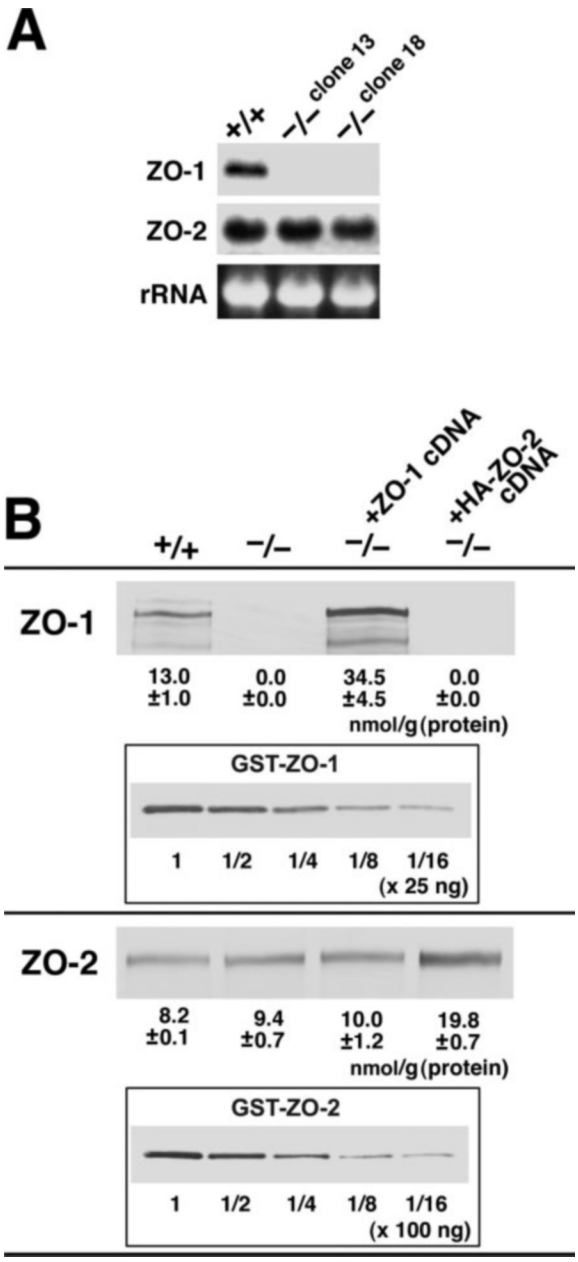

FIG. 10. **Expression levels of ZO-1 and ZO-2.** *A*, Northern blotting. Total RNA was isolated from cells according to the TRIzol method and hybridized with digoxigenin-labeled DNA probes. In *ZO-1*−/− cells (*clones 13* and *18*), the mRNA expression of ZO-2 was not up-regulated as compared with *ZO-1*+/+ cells. *B*, quantitative analyses by Western blotting of *ZO-1*+/+ cells (+/+), *ZO-1*−/− cells (*clone 18*) (−/−), *ZO-1*−/− cells expressing exogenous ZO-1 (−/− + *ZO-1 cDNA*), and *ZO-1*−/− cells expressing HA-ZO-2 (−/− + *HA-ZO-2 cDNA*). GST fusion proteins with a part of ZO-1 and ZO-2 were produced in *E. coli* and purified. The intensity of immunoblotted ZO-1 and ZO-2 in whole cell lysates (*upper* and *lower panels*, respectively) was compared with that of immunoblotted bands of various amounts of the respective GST fusion proteins (in *boxes*). *ZO-1*+/+ cells expressed 13.0 ± 1.0 nmol of ZO-1 and 8.2 ± 0.1 nmol of ZO-2/1 g of total protein (mean ± S.E.). In *ZO-1*−/− cells, ZO-2 was not increased in amount (9.4 ± 0.7 nmol/g) and exogenous ZO-1 was expressed at a level of 34.5 ± 4.5 nmol/g. In *ZO-1*−/− cells expressing HA-ZO-2, the total amount of endogenous ZO-2 and HA-ZO-2 was 19.8 ± 0.7 nmol/g, which was comparable with the total amount of endogenous ZO-1 and ZO-2 in *ZO-1*+/+ cells (~21 nmol/g).

which can directly bind to PDZ domains, and that TJ strands strongly attract various PDZ domain-containing proteins such as ZO-1 and ZO-2 (5). In *ZO-1*−/− cells, a ZO-1 deficiency may leave more space for ZO-2 on the cytoplasmic surface of TJ strands to be recruited from the cytoplasm.

The second characteristic alteration observed in *ZO-1*−/− cells was that cingulin became undetectable at TJs. This was confirmed by the use of two distinct anti-cingulin mAbs. Cingulin has been identified and examined as a component of the TJ plaque structure (15, 43), but knowledge of its physiological functions is still fragmentary. In *ZO-1*−/− cells, the mRNA or protein level of cingulin did not appear to be down-regulated, indicating that ZO-1 is indispensable for cingulin to be recruited to TJs. This finding is consistent with previous reports that cingulin directly binds to ZO-1 *in vitro* (44, 45) but appears to be contradictory to a report that cingulin lacking its "ZO-1 binding motif" still targets to TJs (45), although it is likely that there is another ZO-1-binding domain on cingulin or that there is another indirect molecular linkage between cingulin and ZO-1 via some protein. ZO-2 was also reported to associate directly with cingulin *in vitro* (44), but our present findings favor the notion that ZO-2 does not recruit cingulin to TJs within cells. Although it might be premature to discuss further the behavior of cingulin in *ZO-1*−/−cells, it would be intriguing if in the future *ZO-1*−/− cells could be compared with epithelial cells specifically lacking the expression of cingulin.

TABLE I
Expression levels of ZO-1 and ZO-2

	ZO-1	ZO-2	ZO-1 + ZO-2
			nmol/g total protein
+/+	13.0	8.2	21.2
−/− Clone 18	0.0	9.4	9.4
−/− + ZO-1 cDNA	34.5	10.0	44.5
−/− + HA-ZO-2 cDNA	0.0	19.8	19.8

The third alteration observed in *ZO-1*−/− cells, which would be the most important feature from the viewpoint of epithelial polarization, was that the TJ formation was significantly retarded when the epithelial polarization was initiated by the Ca^{2+} switch. Judging from the immunofluorescence staining and cell aggregation assay, in *ZO-1*−/− cells, the formation of AJs at the initial phase of epithelial polarization did not appear to be affected. The process of TJ assembly, *i.e.* the recruitment of claudins/occludin to the newly formed belt-like AJs, appeared to take significantly longer time in *ZO-1*−/− cells than in *ZO-1*+/+ cells. The retardation of the establishment of the TJ barrier was confirmed by the tracer permeability assay. However, it should be emphasized that, when *ZO-1*−/− cells were cultured for a long time under confluent conditions, they became highly polarized with well organized junctions, which were structurally and functionally indistinguishable from those in *ZO-1*+/+ cells. The question has naturally arisen as to what is the molecular mechanism behind this peculiar feature of *ZO-1*−/− cells, *i.e.* the retardation of TJ formation during epithelial polarization.

ZO-1, ZO-2, and ZO-3 have been speculated to be functionally redundant. Because it was not expressed in detectable amount in Eph4 cells, we did not need to discuss ZO-3. Considering that the cytoplasmic ZO-2 was recruited to TJs instead of ZO-1 in *ZO-1*−/− cells, the following mechanism seems logical. ZO-2 shares the same function as ZO-1, but in *ZO-1*−/− cells due to an insufficient amount of ZO-2, it cannot fully compensate for the ZO-1 deficiency, resulting in a retardation of TJ formation. However, detailed quantitative analyses indicated that the functional relationship between ZO-1 and ZO-2 was not so simple (Table I). Parental *ZO-1*+/+ cells expressed ~13 nmol/g ZO-1 and ~8 nmol/g ZO-2. In *ZO-1*−/− cells, the expression of ZO-2 was not up-regulated. When ZO-1 was exogenously expressed in *ZO-1*−/− cells, the formation of TJs was completely rescued. By contrast, in *ZO-1*−/− cells expressing ZO-2 exogenously, the total amount of exogenous and endogenous ZO-2 (~20 nmol/g) was nearly equal to the total amount of endogenous ZO-1 and ZO-2 (~21 nmol/g) in *ZO-1*+/+ cells, but the TJ assembly was still markedly retarded. Therefore, ZO-1 and ZO-2 would function redundantly to some extent in junction formation/epithelial polarization, but it can be said that they are not functionally identical.

In this study, by conventional homologous recombination, we have for the first time established cultured Eph4 epithelial cells in which the expression of ZO-1 was completely and stably suppressed. It is time-consuming to knock out genes in cultured epithelial cells, but once such knock-out cells are obtained, they are very useful not only for the detailed analyses of phenotypic changes but also for biochemical analyses. However, as numerous molecules are expected to be involved in junction formation/epithelial polarization in a very complicated manner (18, 46–48), further generation of Eph4 cells lacking the expression of various genes will be required. For example, Eph4 cells lacking the expression of ZO-2 or both ZO-1 and ZO-2 would provide crucial information on the functions of ZO-1/ZO-2 when analyzed in combination with *ZO-1*−/− cells. The generation of *ZO-1*−/− cells in this study is just a first step. We are conducting further studies along this line.

Acknowledgments—We thank all of the members of our laboratory (Department of Cell Biology, Faculty of Medicine, Kyoto University) for helpful discussions.

REFERENCES

1. Farquhar, M. G., and Palade, G. E. (1963) *J. Cell Biol.* **17,** 375–412
2. Schneeberger, E. E., and Lynch, R. D. (1992) *Am. J. Physiol.* **262,** L647–L661
3. Anderson, J. M., and Van Itallie, C. M. (1995) *Am. J. Physiol.* **269,** G467–G475
4. Balda, M. S., and Matter, K. (1998) *J. Cell Sci.* **111,** 541–547
5. Tsukita, S., Furuse, M., and Itoh, M. (2001) *Nat. Rev. Mol. Cell. Biol.* **2,** 285–293
6. Staehelin, L. A. (1974) *Int. Rev. Cytol.* **39,** 191–283
7. Furuse, M., Fujita, K., Hiiragi, T., Fujimoto, K., and Tsukita, S. (1998) *J. Cell Biol.* **141,** 1539–1550
8. Tsukita, S., and Furuse, M. (1999) *Trends Cell Biol.* **9,** 268–273
9. Furuse, M., Hirase, T., Itoh, M., Nagafuchi, A., Yonemura, S., Tsukita, S., and Tsukita, S. (1993) *J. Cell Biol.* **123,** 1777–1788
10. Martin-Padura, I., Lostaglio, S., Schneemann, M., Williams, L., Romano, M., Fruscella, P., Panzeri, C., Stoppacciaro, A., Ruco, L., Villa, A., Simmons, D., and Dejana, E. (1998) *J. Cell Biol.* **142,** 117–127
11. Kowalczyk, A. P., Bomslaeger, E. A., Norvell, S. M., Palka, H. L., and Green, K. J. (1999) *Int. Rev. Cytol.* **185,** 237–302
12. Perez-Moreno, M., Jamora, C., and Fuchs, E. (2003) *Cell* **112,** 535–548
13. Mitic, L. L., and Anderson, J. M. (1998) *Annu. Rev. Physiol.* **60,** 121–142
14. González-Mariscal, L., Betanzos, A., and Avila-Flores, A. (2000) *Semin. Cell Dev. Biol.* **11,** 315–324
15. Citi, S., Sabanay, H., Jakes, R., Geiger, B., and Kendrick-Jones, J. (1988) *Nature* **333,** 272–276
16. Keon, B. H., Schafer, S., Kuhn, C., Grund, C., and Franke, W. W. (1996) *J. Cell Biol.* **134,** 1003–1018
17. Balda M. S., and Matter, K. (2000) *EMBO J.* **19,** 2024–2033
18. Ohno, S. (2001) *Curr. Opin. Cell Biol.* **13,** 641–648
19. Benais-Pont, G., Punn, A., Flores-Maldonado, C., Eckert, J., Raposo, G., Fleming, T. P., Cereijido, M., Balda, M. S., and Matter, K. (2003) *J. Cell Biol.* **160,** 729–740
20. Stevenson, B. R., Siliciano, J. D., Mooseker, M. S., and Goodenough, D. A. (1986) *J. Cell Biol.* **103,** 755–766
21. Gumbiner, B., Lowenkopf, T., and Apatira, D. (1991) *Proc. Natl. Acad. Sci. U. S. A.* **88,** 3460–3464
22. Balda, M. S., Gonzalez-Mariscal, L., Matter, K., Cereijido, M., and Anderson, J. M. (1993) *J. Cell Biol.* **123,** 293–302
23. Itoh, M., Nagafuchi, A., Yonemura, S., Kitani-Yasuda, T., Tsukita, S., and Tsukita, S. (1993) *J. Cell Biol.* **121,** 491–502
24. Willott, E., Balda, M. S., Fanning, A. S., Jameson, B., Van Itallie, C., and Anderson, J. M. (1993) *Proc. Natl. Acad. Sci. U. S. A.* **90,** 7834–7838
25. Jesaitis, L. A., and Goodenough, D. A. (1994) *J. Cell Biol.* **124,** 949–961
26. Haskins, J., Gu, L., Wittchen, E. S., Hibbard, J., and Stevenson, B. R. (1998) *J. Cell Biol.* **141,** 199–208
27. Itoh, M., Furuse, M., Morita, K., Kubota, K., Saitou, M., and Tsukita, S. (1999) *J. Cell Biol.* **147,** 1351–1363
28. Furuse, M., Itoh, M., Hirase, T., Nagafuchi, A., Yonemura, S., Tsukita, S., and Tsukita, S. (1994) *J. Cell Biol.* **127,** 1617–1626
29. Fanning, A. S., Jameson, B. J., Jesaitis, L. A., and Anderson, J. M. (1998) *J. Biol. Chem.* **273,** 29745–29753
30. Bazzoni, G., Martinez-Estrada, O. M., Orsenigo, F., Cordenonsi, M., Citi, S., and Dejana, E. (2000) *J. Biol. Chem.* **275,** 20520–20526
31. Itoh, M., Sasaki, H., Furuse, M., Ozaki, H., Kita, T., and Tsukita, S. (2001) *J. Cell Biol.* **154,** 491–497
32. Wittchen, E. S., Haskins, J., and Stevenson, B. R. (1999) *J. Biol. Chem.* **274,** 35179–35185
33. Itoh, M., Nagafuchi, A., Moroi, S., and Tsukita, S. (1997) *J. Cell Biol.* **138,** 181–192
34. Ryeom, S. W., Paul, D., and Goodenough, D. A. (2000) *Mol. Biol. Cell* **11,** 1687–1696
35. Yu, J. Y., DeRuiter, S. L., and Turner, D. L. (2002) *Proc. Natl. Acad. Sci. U. S. A.* **99,** 6047–6052
36. Reichmann, E., Ball, R., Groner, B., and Friis, R. R. (1989) *J. Cell Biol.* **108,** 1127–1138
37. Inoko, A., Itoh, M., Tamura, A., Matsuda, M., Furuse, M., and Tsukita, S. (2003) *Genes Cells* **8,** 837–845
38. Hayashi, K., Yonemura, S., Matsui, T., Tsukita, S., and Tsukita, S. (1999) *J. Cell Sci.* **112,** 1149–1158
39. Yonemura, S., Itoh, M., Nagafuchi, A., and Tsukita, S. (1995) *J. Cell Sci.* **108,** 127–142
40. Adams, C. L., Nelson, W. J., and Smith, S. J. (1996) *J. Cell Biol.* **135,** 1899–1911
41. Asakura, T., Nakanishi, H., Sakisaka, T., Takahashi, K., Mandai, K., Nishimura, M., Sasaki, T., and Takai, Y. (1999) *Genes Cells* **4,** 573–581
42. Ando-Akatsuka, Y., Yonemura, S., Itoh, M., Furuse, M., and Tsukita, S. (1999) *J. Cell. Physiol.* **179,** 115–125
43. D'Atri, F., and Citi, S. (2002) *Mol. Membr. Biol.* **19,** 103–112
44. Cordenonsi, M., D'Atri, F., Hammar, E., Parry, D. A., Kendrick-Jones, J., Shore, D., and Citi, S. (1999) *J. Cell Biol.* **147,** 1569–1582
45. D'Atri, F., Nadalutti, F., and Citi, S. (2002) *J. Biol. Chem.* **277,** 27757–27764
46. Tepass, U., Tanentzapf, G., Ward, R., and Fehon, R. (2001) *Annu. Rev. Genet.* **35,** 747–784
47. Roh, M. H., and Margolis, B. (2003) *Am. J. Physiol.* **285,** F377–F387
48. Nelson, W. J. (2003) *News Physiol. Sci.* **18,** 143–146
49. Saitou, M., Fujimoto, K., Doi, Y., Itoh, M., Fujimoto, T., Furuse, M., Takano, H., Noda, T., and Tsukita, S. (1998) *J. Cell Biol.* **141,** 397–408